RSC Advances

PAPER

CrossMark
click for updates

Reduced graphene oxide supported Ni nanoparticles: a high performance reusable heterogeneous catalyst for Kumada–Corriu cross-coupling reactions†

Koushik Bhowmik,‡[a] Debasish Sengupta,‡[b] Basudeb Basu*[b] and Goutam De*[a]

Reduced graphene oxide (RGO) has emerged as an excellent 2D catalyst support. A high concentration of air stable Ni(0) nanoparticles (~40 wt%) of average size 11 nm can be loaded on reduced graphene oxide. In this article Kumada–Corriu cross-coupling reactions have been studied extensively using RGO supported 40 wt% Ni nanoparticles (Ni/RGO-40) as a heterogeneous catalyst. The reaction conditions were optimized by performing the cross-coupling between 4-iodoanisole and phenylmagnesium chloride in the presence of a catalytic amount of Ni/RGO-40. A detailed study of the catalysis was performed by varying the haloarenes and Grignard reagents under the optimized conditions with yields of 91–72%. The products were characterized by ^1H and ^{13}C NMR spectroscopy. The catalyst was found to be significantly reusable. Finally the recovered Ni/RGO-40 was characterized by X-ray diffraction (XRD) and Raman spectroscopy and found to be unaffected. Considering the catalytic performance, reusability and economic reasons, Ni/RGO-40 can be of technological importance.

1. Introduction

Reduced graphene oxide (RGO) based carbon nanomaterials have attracted immense research interest in the field of catalysis during last few years.[1] The electronic properties[2] and high surface area[3] of RGO opens up new opportunities for its use as a next-generation catalyst or catalyst support.[4,5] The reduced graphene oxide has the more potential to behave as catalyst supports.[6] Because, they can form stable dispersions in aqueous or organic media, and can be blended with other nanomaterials to form nanocomposites.[7] Various metal nanoparticles (NP) have been incorporated in 2D catalyst support RGO to synthesize potential catalyst in different reactions. In recent literatures RGO supported Pd, Au and Pt have been used in organic reactions as catalyst.[8–16] It was observed that in most of the papers RGO supported noble metals have been used as catalyst.

[a]Nano-Structured Materials Division, CSIR – Central Glass and Ceramic Research Institute, 196, Raja S. C. Mullick Road, Kolkata 700032, India. E-mail: gde@cgcri.res.in; basu_nbu@hotmail.com

[b]Department of Chemistry, North Bengal University, Darjeeling-734013, India

‡ These two authors have contributed equally in this work.

Surprisingly there are very few reports on RGO supported low cost first row transition metals as potential catalyst in different organic reactions.[17–19]

In the recent years, RGO as the catalyst support has shown some significant advantages in the area of cross-coupling chemistry. Usually organic ligand-stabilized zero valent homogeneous complexes are used as catalysts in cross-coupling reactions.[20–23] The drawbacks regarding the recovery and reusability of a homogeneous catalyst was overcome by using RGO-supported ligand-free heterogeneous catalysts. The C–C cross-coupling reactions, such as Mizoroki–Heck, Sonogashira and Suzuki–Miyaura, have been successfully catalysed by heterogeneous Pd/RGO composite materials.

The Kumada–Corriu cross-coupling reaction is frequently used to synthesize functionalized biaryls.[24–26] This reaction has the major advantage over Suzuki–Miyaura and Mizoroki-Heck reactions because all aromatic halides including sp^2 C–F can undergo cross coupling with Grignard reagent.[27] In this reaction, the catalyst undergoes a fundamental catalytic cycle involving oxidative addition to a reactive substrate, transmetalation with a Grignard reagent, and reductive elimination to form a carbon–carbon bond. The Ni-catalyzed cross-coupling between aryl halide and Grignard reagent is notable for being among the first cross-coupling reaction reported concurrently by Kumada and Corriu in 1972. Several modifications including Pd-catalyzed conditions and variations in the use of ligands have been developed over the years,[28] and the Kumada–Corriu cross-coupling continues to enjoy many synthetic applications

both in the laboratory as well as in industries. The reaction can be carried out over a wide range of temperatures from $-20\,^{\circ}C$ to refluxing solvents; however, for industrial competence a room temperature reaction is preferable.

Recently, we developed a strategy to stabilize high amount of metallic Ni NP in ambient condition by using RGO as support (Ni/RGO), characterized the composite and used as a potential redox material rather than a catalyst to convert Cr(VI) to Cr(III) in a short period of time at room temperature.[29] Here Ni/RGO took part in the redox reaction and facilitated the reaction rate and at the end of the reaction it was found that the surface of Ni NP got oxidized to Ni^{+2}. Therefore we did not claim this material as a true heterogeneous catalyst. Since there are few studies pertaining to Ni(0) catalysts on heterogeneous supports, we envisaged that the catalytic activity of the Ni/RGO might be explored in various organic reactions. In this paper, 40 wt% Ni(0) nanoparticles loaded in RGO has been focused as a potential heterogeneous catalyst with excellent reusability in Kumada–Corriu cross-coupling reaction. The results are not only encouraging to establish a new RGO-based Ni(0) catalyst, but also pave the way to replace the alternative Pd-based expensive catalysts.

2. Experimental section

2.1 Materials

The following chemicals were used as received. Synthetic graphite powder (particle size <20 μm), sodium nitrate, Grignard reagents and other chemicals were purchased from Sigma-Aldrich, India. Concentrated sulfuric acid, 30% hydrogen peroxide, potassium permanganate and $NiCl_2 \cdot 6H_2O$ were supplied by Merck. Hexamethylenetetramine (HMT) was obtained from Spectrochem Pvt. Ltd. For column chromatography, silica (60–120 μm) (SRL, India) was used. For Thin layer chromatography (TLC), plates (Merck) coated with silica gel 60, F_{254} were used. High pure water (18 MΩ) was used as solvent (Milli-Q System).

2.2 Characterizations

^{1}H and ^{13}C NMR spectra were taken in $CDCl_3$ using Bruker Avance AV-300 spectrometer operating at 300 MHz and 75 MHz respectively. Chemical shifts are reported relative to tetramethylsilane served as internal standard (δ 0 ppm). ^{13}C NMR spectra were recorded with complete proton decoupling and chemical shifts are reported in ppm with the solvent resonance as the internal standard ($CDCl_3$: δ 77.00 ppm). X-ray diffraction (XRD) and Raman studies of the powder samples were performed with Rigaku SmartLab X-ray diffractometer operating at 9 kW (200 mA; 45 kV) using Cu-Kα radiation and Renishaw In Via micro Raman spectrometer, respectively.

2.3 Synthesis of Ni/RGO composite

The synthesis was done following our previously published method.[29] To synthesize about 1 g Ni/RGO composite sample with 40 wt% Ni loading the following method has been followed. 3.75 g of graphene oxide (GO) was ultrasonically dispersed in 800 mL of water. $NiCl_2 \cdot 6H_2O$ (8.75 mmol) and HMT (17.5 mmol) were dissolved in 600 and 250 mL of water, respectively, in two separate flasks. The molar ratio of HMT to $NiCl_2$ was maintained at 2 : 1. All three solutions were mixed together in a round-bottomed flask, stirred for 10 min, and finally sealed in a 2 L Teflon-lined stainless steel autoclave for hydrothermal reaction at 120 °C for 4 h to obtain a $Ni(OH)_2$-embedded GO composite [$Ni(OH)_2$-GO]. The black powder was washed several times with water to remove excess Ni salt and HMT and dried. The powder was then heated in air to 380 °C for 1 h to obtain NiO NP-embedded RGO sheets. *In situ* reduction of NiO NP in the presence of RGO at 350 °C with a continuous flow of H_2 gas (10% H_2-balance N_2) yielded Ni/RGO composite containing 40 wt% Ni NP. This sample is designated as Ni/RGO-40. For control experiments Ni/RGO-60 (60 wt% Ni) and Ni/RGO-20 (20 wt% Ni) were also prepared following the above method. Bare Ni NP was prepared following the method available in the literature.[30]

2.4 Representative procedure of Kumada–Corriu cross-coupling reactions

A mixture of 4-iodoanisole (234 mg, 1 mmol) and Ni/RGO-40 catalyst (14.7 mg, Ni content: 0.1 mmol) in freshly distilled THF (2 mL) under N_2 atmosphere was prepared. Then a solution of PhMgCl (1 mL, 25 wt% in THF, 1.84 mmol) was added dropwise at room temperature (25 °C) with gentle magnetic stirring. The progress of the reaction was monitored by TLC. After completion of the reaction, dry and distilled ethyl acetate (3 mL) was added, stirred gently and then allowed to stand. The supernatant liquid was carefully decanted in another flask and this process was repeated three times more. The combined washings (organic part) were washed with water, dried over anhydrous Na_2SO_4, concentrated and the residue was purified by column chromatography over silica gel. Elution with light petroleum afforded 4-methoxybiphenyl (164 mg, 89%) as white crystalline solid. The product was characterized by ^{1}H and ^{13}C-NMR spectral data, and also compared with reported melting point. A comparison of the ^{13}C peaks of sp^2-C attached to iodide (in 4-iodoanisole) and that of 4-methoxybiphenyl confirms complete conversion through Kumada–Corriu C–C cross-coupling reaction (Fig. S1, ESI†).

2.5 Recovery of the Ni/RGO-40 catalyst

After the reaction of aryl halide (1 mmol) and Grignard reagent (1.8 mmol) in the presence of catalytic Ni/RGO-40 for the time period as mentioned in Table 2, dry and distilled ethyl acetate (3 mL) was added to the reaction mixture and stirred at room temperature for 5 min. The reaction mixture was allowed to settle down and the supernatant liquid was decanted. The process was repeated three times and then water (1 mL) was added to the catalyst containing reaction mixture. The mixture was extracted with ethyl acetate (5 mL) and the aqueous part was separated out, evaporated to dryness using rotary evaporator and dried under vacuum to get free flowing powder.

3. Results and discussion

We have reported the synthesis of Ni/RGO-40 composite powder recently. Detailed characterization revealed high surface area of the composite (125 m^2 g^{-1}) and existence of highly concentrated but separated Ni NP (40 wt%) of average size ~11 nm on the RGO surface. In general, bare Ni NP is very unstable and prone to oxidation in air, but in the Ni/RGO-40 composite, Ni NP can be stabilized by RGO. The RGO surface contains many free electrons[31] and these free electrons help to stabilize the Ni in its zero-valent state. Because of this kind of electronic environment, the metallic Ni NP resides on the RGO surface in tightly bound condition and do not get oxidized. Also, the high surface area and planer structure of RGO prevent the Ni NP from agglomeration into larger particles. As a result, we could load very high Ni loading (40 wt%) in Ni/RGO-40 without any agglomeration.

The other carriers such as alumina, silica, clay and charcoal do not have the electronic property like RGO. Therefore they could not resist the oxidation of Ni NPs during prolonged storage of the catalyst in ambient condition. The loading of Ni NP is also low (1–5 wt%) in other carriers.[32,33] In another approach, precious carrier like phosphine-based dendrimers was used to obtain stabilized Ni NP with low loading of Ni.[34] Inspired by the previous findings Ni/RGO-40 has been tested as a new catalyst in Kumada–Corriu cross-coupling reactions. The schematic representation of Ni/RGO-40 catalyzed Kumada–Corriu cross-coupling reaction is shown in Fig. 1. Here Ni NP is the active catalyst on electron rich RGO support. Further, the planner structure of RGO with high surface area suppresses the agglomeration of Ni NP and provides the sufficient adsorption site to the reacting molecules.[29] It can be noted here that we also prepared Ni/RGO-60, Ni/RGO-20 and bare Ni NP to compare the

catalytic performance with Ni/RGO-40. However, we observed much better catalytic performance of Ni/RGO-40. The reason and a set of comparative results using a representative reaction are given in the ESI (see Section S1, Fig. S2 and Table S1†). For this reason, detailed catalytic experiments were carried out with the optimized sample Ni/RGO-40.

3.1 Optimization of the reaction condition

Initially, we optimized the reaction condition by performing the cross-coupling between 4-iodoanisole and phenylmagnesium chloride (PhMgCl) in the presence of catalytic amounts of Ni/RGO-40 (0.05 and 0.1 mmol with respect to 1 mmol of 4-iodoanisole) in different solvent system. The reaction was indeed successful as we obtained the desired biphenyl in 81–89% isolated yields. Further, variations in the solvent, temperature and quantity of the catalysts did not produce any appreciable changes in terms of the isolated yield of the biphenyl. The optimization of reaction conditions has been presented in Table 1. The entry 2 in Table 1 represents the optimized reaction conditions.

3.2 Kumada–Corriu cross-coupling by varying the ArX (X = I, Br, Cl, F) and ArMgX (X = Br, Cl)

Following the optimized reaction condition we carried out similar cross-coupling reactions on varying the combination of aryl halide (ArX) and Grignard reagent. The results are presented in Table 2. The 3-iodoanisole (Table 2; entry 2) and 2-iodoanisole (Table 2; entry 3) successfully react with PhMgCl and produced the corresponding biphenyl derivatives in 85 and 77% yields, respectively. The feasibility of the reaction between other iodoarenes and Grignard reagents (ArMgX) were also undertaken to obtain the corresponding biaryls. We observed that the *p*-methyliodobenzene (Table 2; entry 4) and iodobenzene (Table 2; entry 5) were successfully reacted with *para* and *meta* isomer of methoxyphenylmagnesium bromide, respectively to produce the corresponding biaryls with a high yield. Similar cross-coupling were performed on different bromo- and chloro- arenes and resulting biaryls were isolated in 80–88% yields (Table 2; entries 6–9).

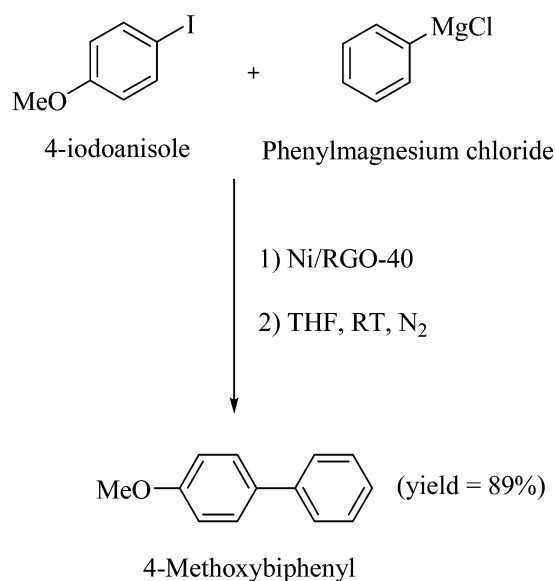Multiple cross-couplings were experienced with diiodo-, bromoiodo-, chloroiodo- and fluoroiodo-benzenes using excess

Fig. 1 Schematic representation of Kumada–Corriu cross-coupling reaction between 4-iodoanisole and phenylmagnesium chloride at room temperature (25 °C) in presence of Ni/RGO-40 as catalyst.

Table 1 Optimization of Kumada–Corriu cross-coupling reaction conditions using Ni/RGO-40 as the catalyst[a]

Entry	Solvent	Catalyst [Ni content (with respect to 4-iodo-anisole) (mmol)]	Temperature (°C)	Time (h)	Yield[b] (%)
1	THF	0.05	25	6	81
2	THF	0.1	25	4	89
3	THF	0.1	40	4	88
4	THF	0.1	60	4	91
5	Dioxane	0.1	25	6	84

[a] 4-Iodoanisole (1 mmol), PhMgCl (1 mL, 25 wt% in THF, 1.84 mmol), solvent (2 mL), under N$_2$. [b] Isolated yield.

Table 2 Kumada–Corriu cross-coupling reaction of halo-arenes with Grignard reagents in the presence of catalyst (Ni/RGO-40)[a]
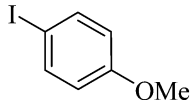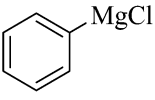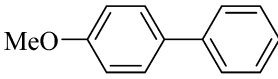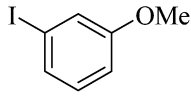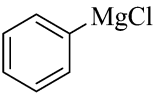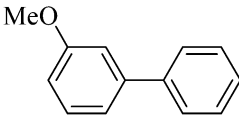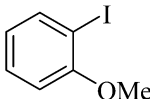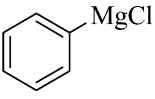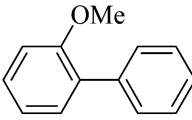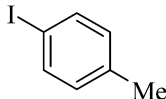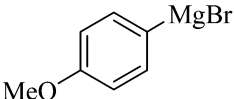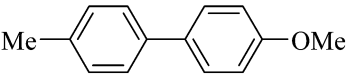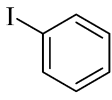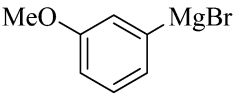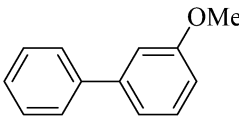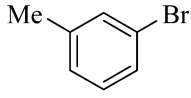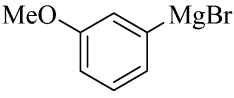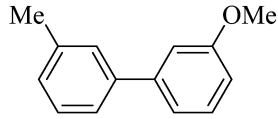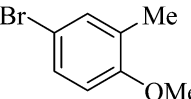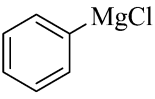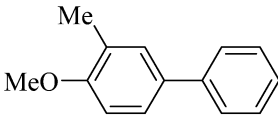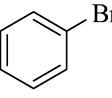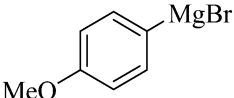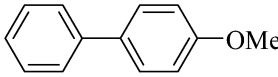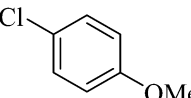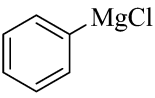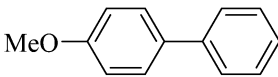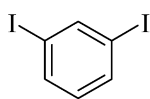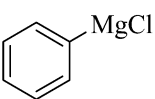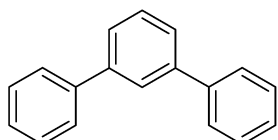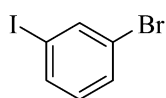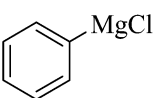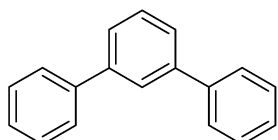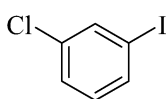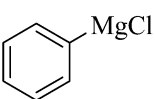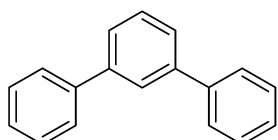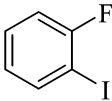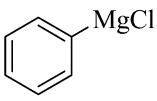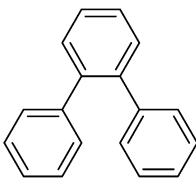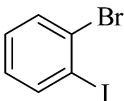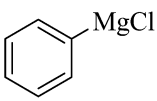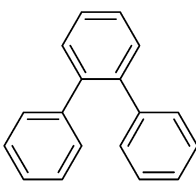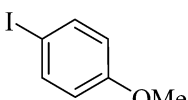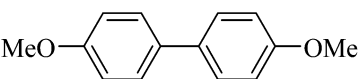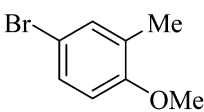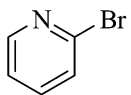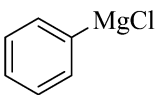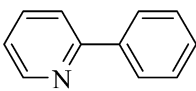
Entry	Aryl Halide (ArX)	Grignard reagent	Time (h)	Product	Yield[b] (%)
1			4		89
2			4		85
3			12		77
4			6		84
5			6		80
6			9		86
7			7		80
8			10		88
9			12		82
10[c]			12		78
11[c]			12		72
12[c]			12		73

Table 2 (Contd.)

Entry	Aryl Halide (ArX)	Grignard reagent	Time (h)	Product	Yield[b] (%)
13[c]			12		76
14[c]			12		73
15			24		76
16			24	—	—
17			10		91

[a] ArX (1 mmol), PhMgCl (1 mL, 1.84 mmol)/ArMgBr (1.5 mmol), Ni/RGO-40 (0.1 mmol), THF (2 mL) stirring at room temperature (25 °C) under N_2.
[b] Isolated yield. [c] PhMgCl (2 mL, 3.68 mmol per mmol of bis-aryl halides).

PhMgCl as the coupling partner in the presence of Ni/RGO-40 (amount of catalyst equivalent to 0.1 mmol Ni was used for 1 mmol haloarene). In each case, we obtained corresponding bis-coupled products (terphenylenes) in good to excellent yields (Table 2; entries 10–14). Thus the present catalytic system was found to be equally active for the oxidative addition to the sp² C–F bond (Table 2, entry 13).

Further, application of the catalyst in Kumada–Corriu cross-coupling was examined with aliphatic Grignard reagent like isopropylmagnesium chloride (i-PrMgCl). Interestingly, the 4-iodoanisole did not couple with the isopropyl group, rather a homo-coupled biphenyl, 4,4′-dimethoxybiphenyl was obtained in appreciable yield (Table 2; entry 15). On the other hand, 2-methyl-4-bromoanisole remained unreacted when treated with i-PrMgCl in THF in the presence of the catalyst (Table 2; entry 16). We presume that there is an exchange reaction between 4-iodoanisole and using i-PrMgCl to generate 4-anisylmagnesium chloride, which then undergoes homo-coupling to produce the 4,4′-dimethoxybiphenyl in 70% yield. Such homo-coupling is however previously known with Fe-catalyzed reactions between aryl halide and Grignard reagent.[35] The scope of the catalytic application has been further broaden with successful cross-coupling with hetero-aryl bromide such as 2-bromopyridine resulting in the formation of 2-phenylpyridine in brilliant yield (Table 2; entry 17).

The NMR spectra of all products (mentioned in Table 2) has been provided in Fig. S3 (ESI†). The melting point of the coupled products was measured and compared with the literature values. The melting point and the characteristic feature of ¹H and ¹³C NMR spectra of different coupled products have been provided in Section S2 (ESI†).

3.3 Reusability of the catalyst

Reusability of a catalyst is an important aspect from the commercial point of view. Reusability increases the potentiality of the catalyst. In order to check the reusability, Ni/RGO-40 was recovered from the reaction mixture, as described above (see Section 2.5). It was used for the next batch of reactions. The recycling experiments were carried out with 4-iodoanisole and PhMgCl and consecutive six runs were performed with appreciable conversion to the coupled product (Fig. 2). In the first cycle, the yield was 89% whereas after six cycles the yield of the product was 77%. The results confirm that the heterogeneous catalyst Ni/RGO-40 is potentially recyclable.

3.4 Characterization of recovered catalyst

After recovery from the reaction mixture the catalyst was characterized by XRD and Raman to confirm that after reaction the oxidation state of Ni remains unchanged. It is noteworthy here
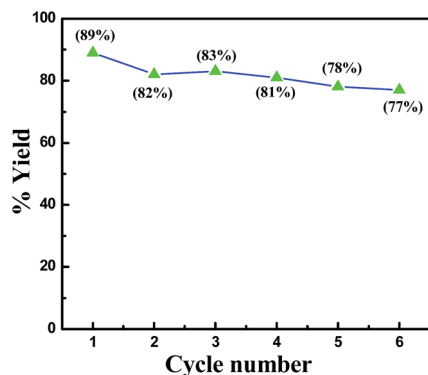
Fig. 2 Reusability of Ni/RGO-40 in consecutive 6 cycles of Kumada–Corriu cross-coupling reaction. The reaction condition was mentioned in Section 2.4 [4-iodoanisole (1 mmol), PhMgCl (1 mL, 25 wt% in THF, 1.84 mmol), solvent (2 mL), under N_2].

that although we tried to eliminate the bi-products (Mg salts formed during the decomposition of Grignard reagent and mixed with the catalyst) by washing (see Section 2.5), the weight of recovered catalyst after the first cycle was found to be higher (22 mg) than the initial weight (14.7 mg). The weight of the recovered catalyst is gradually increasing as the cycles are progressing. The XRD of the recovered Ni/RGO-40 after the first cycle shows clear peaks corresponding to the metallic Ni NPs at 44.49° (111), 51.8° (200) and RGO layers at 25.4° 2θ (Fig. 3). It clearly indicates that the catalyst remains unchanged even after the reaction. However, as mentioned above the recovered catalyst also shows presence of other peaks originated from MgO/
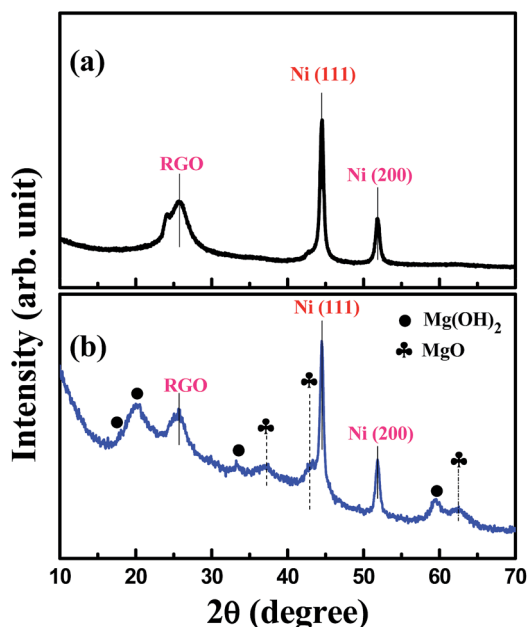

Fig. 3 XRD analysis of Ni/RGO-40: (a) before use as catalyst and (b) recovered catalyst after the first cycle of reaction. The XRD pattern presented in (a) has already been reported in ref. 29, however, to compare with the recovered catalyst this has been recorded again and shown.
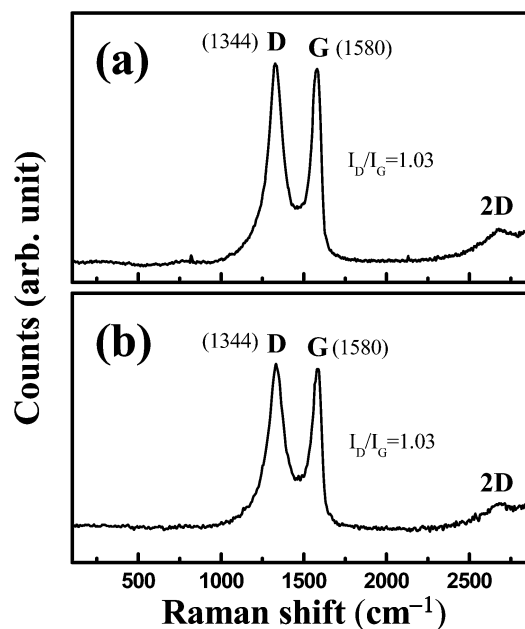

Fig. 4 Raman analysis of Ni/RGO-40: (a) before use as catalyst and (b) recovered catalyst after the first cycle of reaction. The Raman spectrum presented in (a) has already been reported in ref. 29, however, to compare with the recovered catalyst this has been recorded again and shown.

$Mg(OH)_2$ species. The different peaks of $Mg(OH)_2$ and MgO are marked by different symbols in the Fig. 3b. The XRD pattern of recovered catalyst after sixth cycle showed that the intensity of the peaks related to Mg species got increased significantly, however, Ni remains in the metallic state (Fig. S4, ESI†). It is to be noted here that the presence of $MgO/Mg(OH)_2$ in the recovered catalyst did not deteriorate the performance of the catalyst in the subsequent cycles.

The Raman spectrum of the original Ni/RGO-40 catalyst shows the characteristic D (A_{1g} vibrations of the six-membered sp^2 carbon rings[36]) and G (first-order scattering of the E_{2g} mode of sp^2 domains[37]) bands for the composites at 1344 and 1580 cm^{-1}, respectively (Fig. 4a).[29] It was observed that the G band (1580 cm^{-1}) of Ni/RGO-40 exhibited red shifting compared to pure RGO (1595 cm^{-1}, Fig. S5; ESI†). This indicates electron donating effect of RGO[38,39] via a significant electronic interactions between RGO and Ni. The Raman spectrum of recovered Ni/RGO-40 after the first (Fig. 4b) and sixth cycles (Fig. S6; ESI†) did not show any peak related to the oxidized Ni (NiO), and the intensity ratio of D over G band remained same. Therefore it can be concluded that the characteristics of the Ni/RGO-40 in the recovered catalysts remained similar after recycling.

4. Conclusions

An excellent catalytic activity of Ni/RGO-40 in Kumada–Corriu cross-coupling reaction has been established. Cross-coupling between 4-iodoanisole and PhMgCl in the presence of catalytic amount of Ni/RGO-40 produced expected biphenyl compound with a high yield around 89%. The reactions on

varying the haloarene and Grignard reagent also produced the expected coupled product with good to excellent yields. Interestingly, this catalyst was found to be equally active for the oxidative addition to the sp^2 C–F bond. Our results confirmed that Ni/RGO-40 is a promising catalyst as a replacement of Pd-based and other ligand-stabilized homogeneous catalysts. Among notable features, the Ni/RGO-40 would be commercially economical, can overcome the difficulty concerning the recovery from the reaction mixture and was found to be potentially recyclable. Ni/RGO-40 has enough potential as an economic high performance reusable catalyst and can be of technological viability.

Conflict of interest

The authors declare no competing financial interest.

Acknowledgements

Notes and references

1 B. F. Machado and P. Serp, *Catal. Sci. Technol.*, 2012, **2**, 54–75.
2 P. V. Kamat, *J. Phys. Chem. Lett.*, 2010, **1**, 520–527.
3 Y. Gao, D. Ma, C. Wang, J. Guan and X. Bao, *Chem. Commun.*, 2011, **47**, 2432–2434.
4 S. Moussa, A. R. Siamaki, B. F. Gupton and M. S. El-Shall, *ACS Catal.*, 2012, **2**, 145–154.
5 H. Göksu, S. F. Ho, Ö. Metin, K. Korkmaz, A. M. Garcia, M. S. Gültekin and S. Sun, *ACS Catal.*, 2014, **4**, 1777–1782.
6 O. C. Compton and S. T. Nguyen, *Small*, 2010, **6**, 711–723.
7 H. Bai, C. Li and G. Shi, *Adv. Mater.*, 2011, **23**, 1089–1115.
8 G. M. Scheuermann, L. Rumi, P. Steurer, W. Bannwarth and R. Mulhaupt, *J. Am. Chem. Soc.*, 2009, **131**, 8262–8270.
9 Y. Li, X. Fan, J. Qi, J. Ji, S. Wang, G. Zhang and F. Zhang, *Nano Res.*, 2010, **3**, 429–437.
10 Z. Tang, S. Shen, J. Zhuang and X. Wang, *Angew. Chem., Int. Ed.*, 2010, **49**, 4603–4607.
11 A. R. Siamaki, A. E. R. S. Khder, V. Abdelsayed, M. S. El-Shall and B. F. Gupton, *J. Catal.*, 2011, **279**, 1–11.
12 Y. Li, X. B. Fan, J. J. Qi, J. Y. Ji, S. L. Wang, G. L. Zhang and F. B. Zhang, *Mater. Res. Bull.*, 2010, **45**, 1413–1418.
13 E. Yoo, T. Okada, T. Akita, M. Kohyama, I. Honma and J. Nakamura, *J. Power Sources*, 2011, **196**, 110–115.
14 M. Bayati, J. M. Abad, R. J. Nichols and D. J. Schiffrin, *J. Phys. Chem. C*, 2010, **114**, 18439–18448.
15 S. Sharma, A. Ganguly, P. Papakonstantinou, X. Miao, M. Li, J. L. Hutchison, M. Delichatsios and S. Ukleja, *J. Phys. Chem. C*, 2010, **114**, 19459–19466.
16 R. Kou, Y. Shao, D. Wang, M. H. Engelhard, J. H. Kwak, J. Wang, V. V. Viswanathan, C. Wang, Y. Lin, Y. Wang, I. A. Aksay and J. Liu, *Electrochem. Commun.*, 2009, **11**, 954–957.
17 P. Mondal, A. Sinha, N. Salam, A. S. Roy, N. R. Jana and S. M. Islam, *RSC Adv.*, 2013, **3**, 5615–5623.
18 S. O. Moussa, L. S. Panchakarla, M. Q. Ho and M. S. El-Shall, *ACS Catal.*, 2014, **4**, 535–545.
19 Z. Ji, X. Shen, G. Zhu, H. Zhou and A. Yuan, *J. Mater. Chem.*, 2012, **22**, 3471–3477.
20 X. Chen, H. Ke and G. Zou, *ACS Catal.*, 2014, **4**, 379–385.
21 G. A. Molander and O. A. Argintaru, *Org. Lett.*, 2014, **16**, 1904–1907.
22 R. Martin and S. L. Buchwald, *J. Am. Chem. Soc.*, 2007, **129**, 3844–3845.
23 S. Lou and G. C. Fu, *J. Am. Chem. Soc.*, 2010, **132**, 1264–1266.
24 K. Tamao, K. Sumitani and M. Kumada, *J. Am. Chem. Soc.*, 1972, **94**, 4374.
25 R. J. P. Corriu and J. P. Masse, *J. Chem. Soc., Chem. Commun.*, 1972, 144a.
26 N. Liu and Z. X. Wang, *J. Org. Chem.*, 2011, **76**, 10031–10038.
27 N. Yoshikai, H. Matsuda and E. Nakamura, *J. Am. Chem. Soc.*, 2009, **131**, 9590–9599.
28 M. M. Heravi and P. Hajiabbasi, *Monatsh. Chem.*, 2012, **143**, 1575–1592.
29 K. Bhowmik, A. Mukherjee, M. K. Mishra and G. De, *Langmuir*, 2014, **30**, 3209–3216.
30 S. H. Wu and D. H. Chen, *J. Colloid Interface Sci.*, 2003, **259**, 282–286.
31 J. Wang, X. Zhang, Z. Wang, L. Wang and Y. Zhang, *Energy Environ. Sci.*, 2012, **5**, 6885–6888.
32 S. D. Jackson, J. Wills, G. J. Kelly, G. D. McLellan, G. Webb, S. Mather, R. B. Moyes, S. Simpson, P. B. Wells and R. Whymen, *Phys. Chem. Chem. Phys.*, 1999, **1**, 2573–2580.
33 L. Saikia, D. Dutta and D. K. Dutta, *Catal. Commun.*, 2012, **19**, 1–4.
34 L. Wu, J. Ling and Z. Wu, *Adv. Synth. Catal.*, 2011, **353**, 1452–1456.
35 G. Cahiez, C. Chaboche, F. Mahuteau-Betzer and M. Ahr, *Org. Lett.*, 2005, **7**, 1943–1946.
36 A. C. Ferrari, J. C. Meyer, V. Scardaci, C. Casiraghi, M. Lazzeri, F. Mauri, S. Piscane, D. Jiang, K. S. Novoselov, S. Roth and A. K. Geim, *Phys. Rev. Lett.*, 2006, **97**, 187401.
37 C. Fu, G. Zhao, H. Zhang and S. Li, *Int. J. Electrochem. Sci.*, 2014, **9**, 46–60.
38 S. Pisana, M. Lazzeric, C. Casiraghi, K. S. Novoselov, A. K. Geim, A. C. Ferrari and F. Mauri, *Nat. Mater.*, 2007, **6**, 198–201.
39 W. Chan, S. Li, C. Chen and L. Yan, *Adv. Mater.*, 2011, **23**, 5679–5683.